

# Towards Data-Driven Metrics for Social Robot Navigation Benchmarking

Pilar Bachiller-Burgos, Ulysses Bernardet, Luis V. Calderita, Pranup Chhetri, Anthony Francis, Noriaki Hirose, Noé Pérez, Dhruv Shah, Phani T. Singamaneni, Xuesu Xiao and Luis J. Manso

**Abstract**—This paper presents a joint effort towards the development of a data-driven Social Robot Navigation metric to facilitate benchmarking and policy optimization. We provide our motivations for our approach and describe our proposal for storing rated social navigation trajectory datasets. Following these guidelines, we compiled a dataset with 4427 trajectories—182 real and 4245 simulated—and presented it to human raters, yielding a total of 4402 rated trajectories after data quality assurance. We also trained an RNN-based baseline metric on the dataset and present quantitative and qualitative results. All data, software, and model weights are publicly available.

## I. INTRODUCTION

Social robot navigation is becoming an increasingly relevant field, with both growing academic research interest and notable industry involvement. Industrial applications include autonomous vehicles, robots for restaurants and museums, and delivery pods for last mile delivery [15].

Despite efforts of the social robot navigation community to establish principles and guidelines for evaluation [4], benchmarking of social robotics is not yet standardized and can be biased to suit specific research narratives. Social robot navigation (hereafter **SocNav**) is currently assessed through metrics focusing on success, safety, proxemics, or readability [10]. However, different research works consider different metrics depending on what their authors consider relevant and often make claims without considering tradeoffs between metrics or Pareto optimality for the metrics selected.

Furthermore, task type and navigation context [4] are often overlooked. How the type of task affects behavior is exemplified by robots entering people’s personal space, which is required if a robot is delivering an object to a person, but normally should be avoided. The importance of context is exemplified by whether a robot should pass

This work has been submitted to the IEEE for possible publication. Copyright may be transferred without notice, after which this version may no longer be accessible.

This work involved human subjects. Ethics approval was obtained prior to conducting any research from Aston University’s Research Ethics Committee (application nos. EPS21051 and EPS21052).

Pilar Bachiller-Burgos and Luis V. Calderita are with Universidad de Extremadura, Avenida de la Universidad, s/n, Cáceres 10003, Extremadura, Spain. pilarb@unex.es

Luis J. Manso, Ulysses Bernardet and Pranup Chhetri are with Aston University, Birmingham, United Kingdom. l.manso@aston.ac.uk

Anthony Francis is with Logical Robotics, United States of America.

Noriaki Hirose is with University of California Berkeley and TOYOTA Motor North America, United States of America.

Noé Pérez is with Universidad Pablo de Olavide, Spain.

Dhruv Shah is with Princeton University, United States of America.

Phani T. Singamaneni is with LAAS-CNRS, France.

Xuesu Xiao is with George Mason University, United States of America.

bystanders at high speed, which is more appropriate when a robot is carrying urgent medical equipment than when returning to base to recharge, even though the task might be the same from a geometric perspective.

Many existing metrics are computed algorithmically from variables, or *analytic* [4]. Analytic metrics often have poor variable-wise scalability, and disregard factors such as the type of task or contextual factors such as the distribution of objects around the robot. Analytic metrics also frequently lack experimental support showing that what the metric measures matches user perceptions of robot behavior quality. Nevertheless, new metrics continue to be proposed, and, although the intuitions behind them are generally solid, they also often lack empirical support. We argue that metrics should be empirically validated, ideally learned from data, and should evaluate the overall effectiveness and socialness of an entire trajectory. We call such a metric an **All-encompassing Learned Trajectory-wise (ALT)** metric [4]. An ALT metric is learned directly from human evaluations of full robot trajectories, conditioned on context—a category of metrics which, to our knowledge, does not yet exist.

Motivated by the lack of a standardized method to benchmark SocNav policies, limitations of existing analytic metrics, and the absence of an ALT metric, this article studies the feasibility of a data-driven solution to create an ALT metric, which would solve all these problems.

Robots are not yet commonly integrated into everyday human environments with explicit quantitative feedback [20], so few datasets suitable for training learned metrics exist. This gap makes compiling a dataset specifically for this purpose essential. Therefore, this paper contributes with:

- 1) a **specification** for storing social robot navigation trajectories along with their ratings,
- 2) **open-source tools** for visualizing this data,
- 3) a proof-of-concept **dataset** following this spec, and
- 4) a **learned metric** exploiting this dataset.

Our dataset specification includes information concerning the environment, the humans, the robot’s task, its context, and the trajectory of the robot, as well as demographic information about the human raters and the scores for the trajectories they rated. The specification and any dataset that follows it can be exploited for (see Fig.1):

- **Training ALT metrics:** Given a sufficiently large and varied set of trajectory-score pairs, a supervised machine learning model can be trained on the dataset to produce a learned ALT metric.

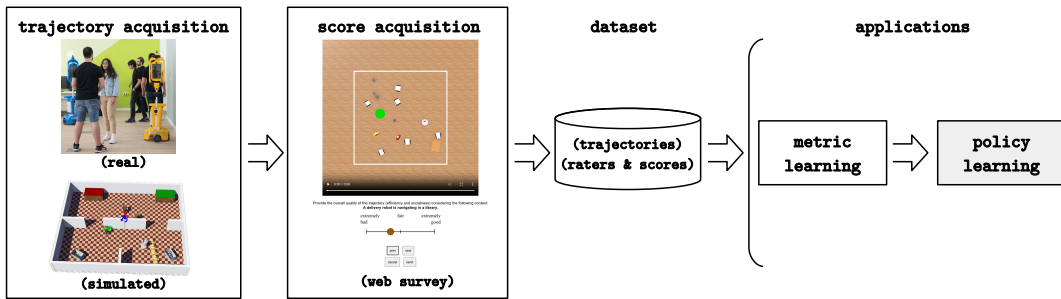


Fig. 1: We acquire trajectories from both real and simulated scenarios. Simulated trajectories have a lower cost and allow for ethical recording of unsafe behavior, but real trajectories are still required to ensure generalisation. We generate a top-down view for each trajectory and show it to raters to collect scores. We have made all the data we collected public, including trajectories, raters’ data, and their ratings. Metric and policy learning are use cases for the dataset.

- **Policy development:** Given a high-quality ALT metric, SocNav policies can be derived by optimizing the score for the metric—for example, using reinforcement learning or model predictive control.

Our proof-of-concept metric shows that an ALT metric can be learned, and encourages the community to help scale the dataset to the point where metrics learned over it can be used as the *de facto* metric for benchmarking robot trajectories<sup>1</sup>. Policy development is out of the scope of this paper.

In addition to our main contributions, we provide experimental results on data quality and the accuracy of our metric, as well as qualitative results for stereotypical scenarios.

## II. RELATED WORK

Regarding **learned SocNav metrics**, SocNav1 [8] and SocNav2 [2] are the initiatives that most closely resemble the goals of the paper at hand. The SocNav1 [8] dataset provides scores of static scenarios including one robot and a variable number of humans, with generic object bounding boxes and explicit interactions (human-to-human and human-to-object). The SocNav2 dataset [2] extended SocNav1 to account for brief periods of time and specific goals, but not full trajectories. Even though these works provide learned SocNav metrics, they are step-wise, *i.e.*, they account for snapshots rather than whole trajectories. Furthermore, none of them consider the context of the tasks.

Although not strictly a metric, another notable research direction estimates the perturbation of pedestrian movement as a variable to minimize [1, 5]. Despite its elegant simplicity, this approach is dependent on the number of people in the environment, and does not account for the context of the task nor the general perception of trajectory quality. Similarly, [13] learns a cost function over observations of real human motion interactions found in publicly available datasets, then uses that cost to determine a navigation controller. While this cost function could be used as a metric, this approach only considers the context of crossing pedestrians on a pavement and has the same shortcomings as [5] and [1].

Many **datasets** relevant to human trajectory modeling exist, but datasets which also include humans, robots and environmental data (such as a map or objects) are scarcer. JRDB [9], THOR [14], SCAND [7] and SACSoN [5] are examples of such datasets. They provide raw sensor data from teleoperated or autonomous robot trajectories, and frequently include a video feed and 3D LiDAR or RGBD data. However, with the exception of THOR [14], pedestrians are annotated as bounding boxes or 2D points *without* orientation.

We found no datasets containing rated robot trajectories, so we chose for this paper to reuse and annotate existing datasets along with recording new additional data. Although THOR initially seemed a good fit for this purpose because it includes object annotations, oriented pedestrians and even human gaze orientation, we chose SACSON instead because of its scale. Nevertheless, as mentioned in the introduction, we combined synthetic data with this real data so we could vary the quality of the trajectories in order to reduce the bias of the learned metric.

## III. DATASET SPECIFICATION AND TOOLS

This section first describes our proposed dataset specification, including the variables it represents and its file format, and then summarizes the software we developed to work with compatible datasets. The design decisions behind this specification are the result of a series of focus group sessions where the authors of the paper participated.

### A. Variables

The dataset comprises variables related to raters, trajectories, and rater-trajectory scores. For every **rater**, the dataset contains their age (integer), gender (categorical: female, male, non-binary, transgender, other, no-answer), country of residence (categorical), and a rating list. Each rating list contains tuples  $(t, c, r)$ , where  $t$  is a trajectory identifier (string),  $c$  is a context (string), and a  $r$  is a **score** (float,  $r \in [0, 1] \subset \mathbb{R}$ ). We chose to acquire real-valued scores rather than a Likert scale following best-practice HRI studies [18] which regard sensitivity as more relevant than repeatability. To score trajectories, the survey tool used a slider with three references “*extremely bad*” (score 0), *fair* (score 0.5)

<sup>1</sup>Instructions to contribute are in the software repository <https://github.com/SocNavData/SocNav3>.

and “*extremely good*” (score 1). Note that contexts are not necessarily bound to trajectories when trajectories are recorded; this enables us to vary the context to explore how different contexts affect the perception of the same trajectory.

**Trajectories** contain data on the robot, the task and its context, humans, objects, and the environment, as shown in Table I. Except for variables related to the task and the environment, which apply to the whole trajectory, variables are recorded with a timestamp at each time step.

The **robot** is described providing its pose (in  $SE(2)$ ), speed (a twist vector), drive system (categorical variable, “differential”, “omnidirectional”, “ackerman”, or “biomimetic”) and shape (circle, rectangle, or a generic polygon described using a vertex representation). The focus group considered whether to add 3D information about the shape of robots or objects. While this could help detect potentially problematic situations (*e.g.*, robot or object geometry impeding the visibility of other agents), most current metrics are very far from considering such aspects. Therefore, the focus group decided not to include 3D shapes in the initial version of the specification.

The **goal** is defined differently depending on the task type, which is provided as a categorical variable “*go-to*”, “*guide-to*”, “*follow*”, or “*interact-with*”. For *go-to* tasks, the specification requires a target 2D position (in meters) and a target angle (in radians), both with thresholds using Euclidean and angular distance, respectively. By varying these threshold values, a *go-to* task can specify a very stringent  $SE(2)$  point target, just a position, or only an angle. Tasks of type *guide-to*, are specified similarly to *go-to* tasks, but require an additional human identifier, and the task target applies to the human, not the robot. Tasks of type *follow* and *interact-with* require a human identifier to specify which human is the robot expected to follow, along with an Euclidean distance threshold.

**Humans** are described with a numerical identifier, their 2D pose and, optionally, the 3D coordinates of their COCO-18 key-points. The focus group decided making the 3D version of the human pose mandatory would limit adoption, as few research groups or even companies have access to full human pose trackers. However, the focus group decided to add 3D human pose as an optional element so the specification would not become prematurely obsolete.

**Objects** are described with an identifier, a text-based description, their 2D pose and their shape (circle, rectangle, or polygon). The focus group chose a text-based description over a predefined set of object types because of its flexibility (text enables open-set objects) and fidelity (language models can often easily turn text into categories, but the reverse is not true without loss of information).

The remaining **environmental** information consists of the walls (specified as 2D polylines), a 2D grid map (with the same fields as ROS2 maps), and area semantics (text-based, following the same rationale as the text-based object description). The grid map is specified with a 2D data array, and the resolution of the grid is specified in metres per cell.

## B. Structure and storage

The raw dataset contains two main directories: one containing the *trajectories* and another one containing data about the raters and their *ratings*.

The *trajectories* directory contains JSON files of recorded trajectories in sub-directories named according to the source of the trajectory data. Each file contains one trajectory, and their relative file paths serve as trajectory identifiers. The data structure of these JSON files is presented in Table I.

The *ratings* directory contains a separate JSON file for each questionnaire completed, as described in III-A. In addition to the rater’s demographic information, each of these files store their ratings as a list of tuples: trajectory identifier (*i.e.*, a relative path to the JSON file), context, score.

## C. Software layer

In the Git repository of the project<sup>2</sup>, we provide scripts to visualize and perform statistical analyses on the data, classes for data-loading, data augmentation and normalization, and code to deploy the surveying tool to acquire ratings.

**Statistical analysis scripts:** Used to compute the quadratic weighted Cohen’s kappa coefficient of the raters and to produce the consistency map in Fig. 4. More details are provided in Sec. IV-B.

**Trajectory visualization tool:** Unlike other types of datasets with simpler datatypes, such as plain text, images, or audio, trajectory data combines different variables, which makes it harder to work with and visualize. Visualization is crucial in this domain because the complexity of the data structures makes errors likely if the trajectories are not carefully compiled. Inconsistencies in coordinate or unit systems are common issues that can be picked up visually early on with the right tools. The visualization tool is shown in 2a. A 3D visualization tool built on top of Webots [11] is also provided to generate video recordings.

**Surveying tool:** Running a ratings survey benefits from a more usable—and aesthetic—representation. The surveying tool shows video recordings along with a randomly generated context, asks raters to provide their scores, as shown in Fig. 3. The trajectories to use, the types of contexts, the maximum number of scores per rater, and the repeated control questions can all be configured.

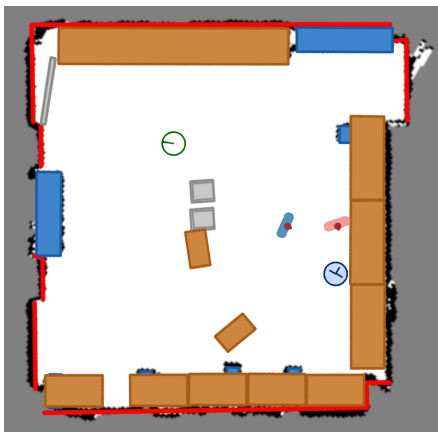
**Data normalization, and augmentation:** Normalization and augmentation help to include equivariances and invariances in machine learning models without embedding them into equations. Applying these transformations to robot trajectories is complex and error-prone, and so, as with visualization, tooling support is helpful. To avoid forcing users to duplicate data augmentation code, and to streamline and homogenize data augmentation and normalization, PyTorch data transforms implementing such features are provided.

Data normalization automatically reframes all poses into the goal frame of reference; this can steer machine learning models towards invariance *w.r.t.* the frame of reference.

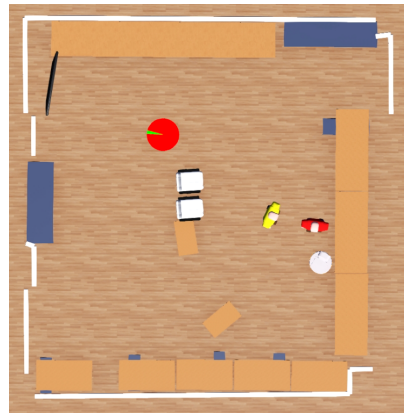
<sup>2</sup><https://github.com/SocNavData/SocNav3>

Type	Variable	Description
Robot	Pose	2D position (m) and orientation (rad) on the plane.
	Speed	Lineal (m/s), angular (rad/s)
	Drive	Categorical (differential/omni/ackerman)
	Shape	2D <i>circle</i> (radius), <i>rectangle</i> (width, height) or <i>polygon</i> (list of points).
Task	Type	Task type, either “go-to”, “guide-to” or “follow”.
	Position + threshold	For go-to and guide-to types of tasks. 2D position + threshold (m).
	Orientation + threshold	For go-to and guide-to types of tasks. 2D orientation + threshold (rad).
	Human identifier	For <i>guide-to</i> and <i>follow</i> types of tasks.
Humans	Context	Textual description of the context, in English.
	Identifier	Integer that uniquely identifies the human in a given episode.
Objects	Pose	2D position (m) and orientation (rad) on the plane.
	Full Pose (optional)	The 3D position of the COCO-18 key point set.
	Identifier	Integer that uniquely identifies the object in a given episode.
	Type	Free text describing the type of the object.
Environment	Pose	2D position (m) and orientation (rad) on the plane.
	Shape	The 2D shape of the object.
	Walls	Sequence of polylines (2D, m).
Environment	Grid	Occupancy map: 2D grid + resolution (m/cell).
	Area semantics	Free text describing the area → e.g., “indoor”, “outdoor”, “kitchen”, “a science museum”.

TABLE I: Data stored per trajectory.



(a) 2D custom representation.



(b) Webots-based 3D representation.

Fig. 2: Trajectory visualization using a custom 2D representation (2a) and 3D simulator (Webots 2b).

The provided software implements three types of data augmentations. First, to enhance robustness to noise, poses can be augmented with additive Gaussian noise. Secondly, when goal orientations exceed a threshold larger or equal to  $\pi$  rad, the orientation value is randomized. Finally, trajectory data can be randomly mirrored (left-right).

#### IV. DESCRIPTION AND ANALYSIS OF THE DATASET PROTOTYPE

We provide a dataset to show how the proposed dataset structure can be exploited to generate a learning-based metric. We collected 4427 trajectories, 182 real and 4245 simulated. We extended this initial set by varying the configuration of the walls in the scenarios of the compiled trajectories (*i.e.*, removing some or all of the walls). This process resulted in a total of 7472 trajectories. It is key to have both real and simulated data sources because they pose different challenges: real trajectories typically have lower variability than simulated ones because of the expense of recording trajectories in multiple scenarios, while simulated data have less realistic movements and noise. Additionally,

due to safety and ethical reasons, dangerous robot trajectories can only be acquired in simulation. Furthermore, acquiring a large enough dataset to cover all possible situations with real data exclusively would be unrealistically expensive.

In this study, we kept cost bounded by limiting this *proof-of-concept* dataset in several ways, nevertheless ensuring good coverage within the selected domain. Firstly, the dataset is limited to indoor areas whose bounding box ranges between 6 m and 10 m wide. The navigation tasks covered in the dataset are all of the type “go-to”; other tasks such as following or guiding humans are left for future additions to the dataset repository. The objects considered in the dataset are limited to chairs, shelves, tables, lights, and plants. The maximum robot speed recorded is 2 m/s.

##### A. Trajectories recorded

Two sources were used to acquire **real trajectories**. A set of 109 trajectories was recorded at ARP laboratory (Aston University). A  $8 \times 7.4$  meters wide room was populated with tables, shelves, chairs, a TV, and from 1 to 6 humans. Another 73 trajectories were re-used from the SACSoN

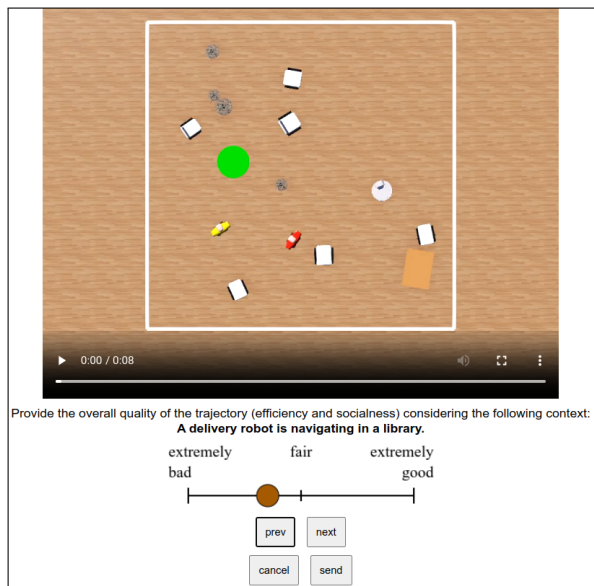


Fig. 3: Survey screenshot.

dataset [5]. The trajectories available in SACSoN were recorded in environments larger than the maximum area set for the proof-of-concept dataset, so they were cropped to comply with the range allowed within the restrictions for our dataset.

We included **simulated trajectories** from a range of simulators and algorithms, using both manual control and a learned RL agent on SocNavGym [6], HATEB [16], and HuNavSim [12], as well as manual control on Gazebo.

### B. Data quality

Each survey included 15 control questions to assess consistency between the participants. Additionally, five of these questions were presented twice to evaluate intra-rater consistency. In total, 49 participants scored 6, 481 trajectories.

To ensure data quality, we first discarded ratings from participants who did not answer all control questions. For the 34 remaining participants, we then applied a selection process that considers both intra-rater and inter-rater consistency using the quadratic weighted Cohen’s kappa coefficient. We define  $\mu_{intraH}$  as a high-quality threshold and  $\mu_{intraL}$  as a minimum-quality threshold for intra-rater consistency and  $\mu_{inter}$  as a minimum threshold for inter-rater consistency. The selection consists of the following steps:

- 1) Compute the average score for each control question over the population of raters with an intra-rater consistency greater than  $\mu_{intraH}$ .
- 2) Discard raters with an intra-rater consistency lower than  $\mu_{intraL}$  or an inter-rater consistency lower than  $\mu_{inter}$  with respect to the average scores of the control questions.

Combining intra- and inter-rater agreements provides more solid results than a separate selection. Due to the limited number of repeated control questions, small variations in the answers of a rater could have a significant impact on

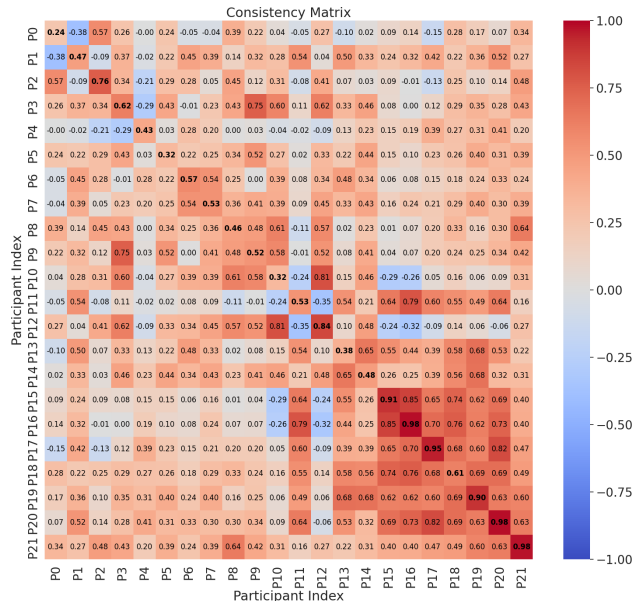


Fig. 4: Consistency map of selected raters.

their intra-rater agreement [19]. Thus, an initial selection based only on high intra-rater consistency could result in discarding too many raters. Using both coefficients, we can retain raters who align with the group opinion, even with minor inconsistencies in their responses. This approach improves the overall reliability and representativeness of the data by filtering out erratic and atypical ratings without being excessively restrictive.

Figure 4 shows the consistency map of the raters selected following the described procedure, considering values of 0.4, 0.1 and 0.2 for  $\mu_{intraH}$ ,  $\mu_{intraL}$  and  $\mu_{inter}$ , respectively. The resulting set of **22 raters** yields a **final dataset of 4402 scored trajectories**.

## V. EXPERIMENTAL RESULTS

We propose a Gated Recurrent Unit-based neural network (GRU [3]) ALT metric model to demonstrate the feasibility of data-driven approaches and to serve as a baseline in future work. This section describes the data transformations applied, the architecture used, the training procedure, as well as quantitative and qualitative results.

### A. Data transformations

The raw trajectory data is augmented using mirroring and transformed into 1D vectors that serve as input to the GRU. The vectors  $(x_0, \dots, x_t, \dots, x_T)$  are the concatenation of trajectory features  $(f_t)$ , metric-based features  $(m_t)$ , and an ad-hoc context embedding  $(c_t)$ :

$$x_t = f_t || m_t || c_t \quad (1)$$

The trajectory features,  $f_t$ , include pose, speed, and acceleration of the robot *w.r.t.* the goal frame of reference, goal thresholds (regarding position and orientation), general scenario information (flags indicating the presence of humans

and the existence of walls), and data that allows contextualizing in time the current step in the whole trajectory (the current step ratio and a last step flag).

The metrics compiled in  $m_t$  are the following:

- A flag indicating whether the robot reaches the goal.
- Distances to the nearest human, object, and wall.
- Flags indicating whether the robot has collided with a human, an object, or a wall.
- Number of humans within a radius of the robot (0.4, 0.6, and 0.8 m).
- Flags indicating social space intrusions, considering the same thresholds as in the previous point.
- Features indicating potential danger to humans: minimum time to collision, maximum *cost of fear*, and maximum *cost of panic* as defined in [17].
- Minimum distance from humans up to the current step.
- Path efficiency ratio measured as the initial distance to the goal divided by the length of the trajectory up to the current step.

The contextual values in  $c_t$  are computed from the free-form text describing the context of the task using queries to an LLM (Anthropic Claude). The prompt used was: “*I will give a task description for a robot. I want you to reply with the percentile (a number from 0 to 100) that corresponds to <VARIABLE> in comparison with that of other tasks you could imagine. I don’t want an explanation, only the percentile. Take your time to think, but respond with a single integer from 0 to 100.*”, where <VARIABLE> is substituted with each of the strings in Table II. The output of the LLM is later normalised to the range 0-1.

Contextual query
the urgency of the task
the importance of the task
the risk involved in the task
the distance the robot should keep to humans during the task
the distance the robot should keep to objects during the task
the speed with which the robot should move
the importance of comfort versus efficiency in the task
to what extent bumping into a human would be justified
to what extent bumping into an object would be justified
the importance of moving in a predictable way

TABLE II: Contextual queries used in the LLM prompts.

### B. Training procedure

After discarding the trajectories used as control questions, we create a 0.9/0.05/0.05 train/validation/test split and train a GRU-based neural network. The network consists of a GRU connected to an MLP. The GRU has 4 layers with 256-unit hidden layers, and the output of the last step of its sequence is fed into an MLP with a 256-unit hidden layer and a 1-unit output layer. The hidden layers use LeakyReLU activation with a 0.01 negative slope, and the output layer uses sigmoid activation. The model is trained with a batch size of 32 and a learning rate of 1e-5, using MSE loss with the target of the raters’ scores. The training follows an early-stopping strategy with a patience of 20 epochs. Checkpoint saving is performed every time the loss of the validation set improves.

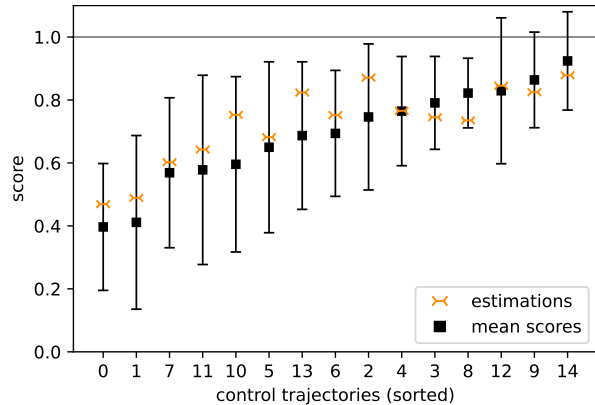


Fig. 5: Plot for the control questions with their corresponding mean, standard deviation, and the estimations made by the model. The control questions are shown sorted according to their mean score.

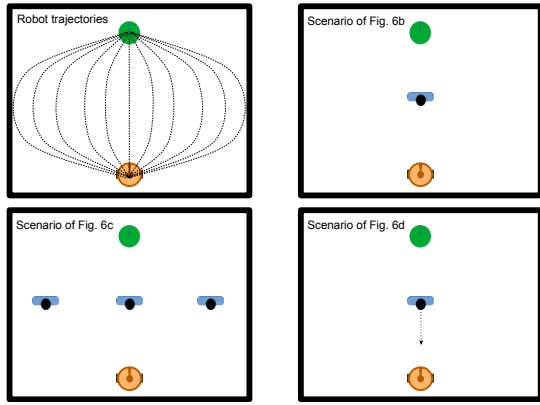
### C. Results

Training resulted in an MSE loss of 0.0469 for the validation dataset, achieved in epoch 208. The final test MSE loss is **0.0477**, equivalent to a MAE of **0.162**. The MSE and MAE of the model with respect to the mean of the control questions were 0.0062 and 0.066, respectively. To avoid over-representing these data points, control questions were not included in the dataset. Fig. 5 shows the mean scores for the control questions, along with their standard deviations, and the estimation the model made for each of them.

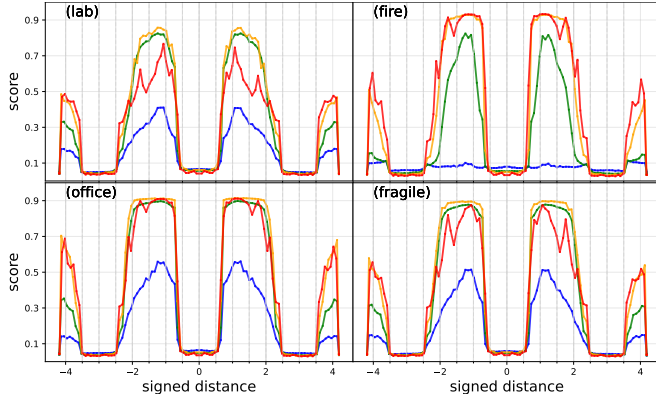
To test the model from a qualitative perspective, we generated three simulated scenarios in which people are located frontally between the robot’s initial position and the goal position (Fig. 6a). The robot moves at different speeds following several trajectories (a total of 101) that deviate a variable distance from the straight line to the goal. The top left image in Fig. 6a shows a subset of these trajectories as dotted lines. Additionally, four different contexts are considered for each scenario, each with distinct urgency, importance, and risk among other variables.

Figures 6b, 6c, and 6d show the metric model output for these three scenarios. The horizontal axis represents the maximum deviation of the trajectory from the straight line. The sign refers to the side, left or right, where the deviation occurs. The plots show the score assigned by the trained model to each trajectory.

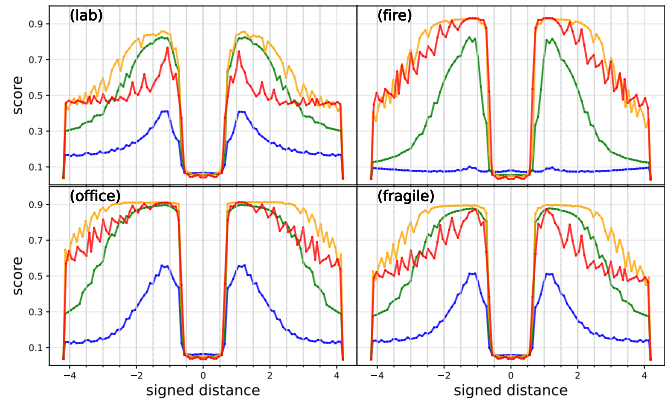
As these figures show, the model learns to distinguish among contexts. The highest speed is penalized more in the contexts labeled as *lab* and *fragile* in Fig. 6, where the robot would generally be expected to move slowly due to the risk of the task. In these two contexts, the robot is also expected to maintain a wider distance from humans, which explains why trajectories closer to the human (*i.e.*, with smaller deviations) receive lower scores than in the other contexts. In contrast, the *fire* context reflects a high-urgency situation: the lowest speed results in scores close to zero on all trajectories and scenarios, and closer proximity to humans is more acceptable.



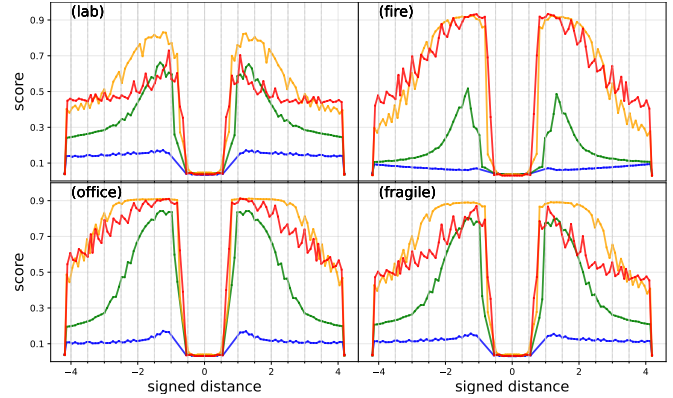
(a) Robot trajectories and scenarios of Figs. 6b, 6c, and 6d.



(c) Three static persons.



(b) One static person.



(d) A person moving in the direction of the robot.

Fig. 6: This figure shows the output of the learned metric for different trajectory variations, situations, contexts and speeds. In all scenarios, the robot and the goal are located in the same position, as indicated in Fig 6a, in orange at the bottom and green at the top, respectively. In Figs. 6b and 6d, there is a single human; in the first case static, in the second case approaching the location where the robot starts. In Fig.6c, there are three humans, as depicted in Fig.6a. To get to its goal the robot follows different trajectories, with varying degrees of divergence from the central line (top-left image of Fig. 6a). The contexts are as shown on the top-left of each figure: (lab) is for “A robot is working with lab samples. The samples contain a deadly virus”; (fire) is for “A restaurant robot is looking for a fire extinguisher, as it just detected a fire”; (office) is for “An office assistant robot keeps track of who is in the office today”, and (fragile) is for “A delivery robot is navigating in a hospital. It works with fragile objects”. Speed is color-coded: — 0.20 m/s — 0.40 m/s — 0.80 m/s — 1.60 m/s.

In addition, in the *office* context, where the task is less critical, the lowest speed is less penalized and the scores decay more slowly than in the other contexts as the robot deviates from the straight line to the goal. In the scenario with three pedestrians (Fig 6c), this behavior is less evident. Nevertheless, it can be observed how, for the range of distances with the highest scores, the *office* context receives practically the same score, while the rest of the contexts are penalized as the deviation increases.

Finally, notable differences can be observed between the two scenarios with one person (Figs. 6b and 6d). When the person moves, the robot should move faster than when the person is static. This aligns with the expectation that the robot should actively maneuver in time to avoid the moving person safely. Additionally, deviating farther from the straight line is more penalized than in the static scenario, which can be explained by the fact that, once the robot has safely avoided the human, the distance from them is greater

than in the stationary person scenario, as the person moves away from the robot.

## VI. CONCLUSIONS AND FUTURE WORK

This paper described how All-encompassing Learned Task-wise metrics [4] can be learned following a data-driven approach in the context of social robot navigation. The experimental results support the idea that the approach is feasible; the quantitative results achieve MSE and MAE of 0.0477 and 0.162, respectively. The qualitative results show that the learned metric is sensitive to both the content of the scenarios and the context of the tasks.

The authors acknowledge these results could be enhanced with additional data and architectural improvements, which points to the need for further research in this area. More sophisticated architectures were not satisfactory in our experiments, arguably due to the size of the dataset.

Our envisioned future work spans two different areas:

a) increasing the dataset size, and b) development of domain-specific deep learning architectures that can more efficiently leverage geometric relationships.

#### REFERENCES

- [1] Subham Agrawal, Nils Dengler, and Maren Bennewitz. “Evaluating Robot Influence on Pedestrian Behavior Models for Crowd Simulation and Benchmarking”. In: *International Conference on Social Robotics*. Springer. 2024, pp. 370–382.
- [2] Pilar Bachiller Burgos, Daniel Rodriguez-Criado, Pablo Bustos, Ronit Jorvekar, Diego Faria, and Luis Manso. “A graph neural network to model disruption in human-aware robot navigation”. In: *Multimedia Tools and Applications* 81 (2022).
- [3] Kyunghyun Cho, Bart Van Merriënboer, Caglar Gulcehre, Dzmitry Bahdanau, Fethi Bougares, Holger Schwenk, and Yoshua Bengio. “Learning phrase representations using RNN encoder-decoder for statistical machine translation”. In: *arXiv preprint arXiv:1406.1078* (2014).
- [4] Anthony Francis et al. “Principles and Guidelines for Evaluating Social Robot Navigation Algorithms”. In: *ACM Transactions on Human-Robot Interaction* 14.2 (2025).
- [5] Noriaki Hirose, Dhruv Shah, Ajay Sridhar, and Sergey Levine. “Sacson: Scalable autonomous control for social navigation”. In: *IEEE Robotics and Automation Letters* 9.1 (2023), pp. 49–56.
- [6] Aditya Kapoor, Sushant Swamy, Pilar Bachiller, and Luis J. Manso. “SocNavGym: a Reinforcement Learning Gym for Social Navigation”. In: *32nd IEEE International Conference on Robot and Human Interactive Communication*. IEEE. 2023, pp. 2010–2017.
- [7] Haresh Karnan, Anirudh Nair, Xuesu Xiao, Garrett Warnell, Sören Pirk, Alexander Toshev, Justin Hart, Joydeep Biswas, and Peter Stone. “Socially compliant navigation dataset (scand): A large-scale dataset of demonstrations for social navigation”. In: *IEEE Robotics and Automation Letters* 7.4 (2022), pp. 11807–11814.
- [8] Luis J. Manso, Pedro Nuñez, Luis V. Calderita, Diego Faria, and Pilar Bachiller. “SocNav1: A dataset to benchmark and learn social navigation conventions”. In: *Data* 5.1 (2020), p. 7.
- [9] Roberto Martín-Martín, Hamid Rezaatofghi, Abhijeet Sheno, Mihir Patel, J. Gwak, Nathan Dass, Alan Federman, Patrick Goebel, and Silvio Savarese. “JRDB: A dataset and benchmark for visual perception for navigation in human environments”. In: *arXiv preprint arXiv:1910.11792* (2019).
- [10] Christoforos Mavrogiannis, Francesca Baldini, Allan Wang, Dapeng Zhao, Pete Trautman, Aaron Steinfeld, and Jean Oh. “Core challenges of social robot navigation: A survey”. In: *ACM Transactions on Human-Robot Interaction* 12.3 (2023).
- [11] Olivier Michel. “Cyberbotics Ltd. Webots: professional mobile robot simulation”. In: *International Journal of Advanced Robotic Systems* 1.1 (2004), p. 5.
- [12] Noé Pérez-Higueras, Roberto Otero, Fernando Caballero, and Luis Merino. “HuNavSim: A ROS 2 Human Navigation Simulator for Benchmarking Human-Aware Robot Navigation”. In: *IEEE Robotics and Automation Letters* (2023).
- [13] Noé Pérez-Higueras, Rafael Ramón-Vigo, Fernando Caballero, and Luis Merino. “Robot local navigation with learned social cost functions”. In: *11th International Conference on Informatics in Control, Automation and Robotics*. Vol. 2. IEEE. 2014, pp. 618–625.
- [14] Andrey Rudenko, Tomasz P Kucner, Chittaranjan S. Swaminathan, Ravi T. Chadalavada, Kai O. Arras, and Achim J. Lilienthal. “THÖR: Human-Robot Navigation Data Collection and Accurate Motion Trajectories Dataset”. In: *IEEE Robotics and Automation Letters* 5.2 (2020), pp. 676–682.
- [15] Phani Teja Singamaneni, Pilar Bachiller-Burgos, Luis J Manso, Anaís Garrell, Alberto Sanfeliu, Anne Spalanzani, and Rachid Alami. “A survey on socially aware robot navigation: Taxonomy and future challenges”. In: *The International Journal of Robotics Research* 43.10 (2024), pp. 1533–1572.
- [16] Phani Teja Singamaneni, Anthony Favier, and Rachid Alami. “Human-aware navigation planner for diverse human-robot interaction contexts”. In: *IEEE/RSJ International Conference on Intelligent Robots and Systems*. IEEE. 2021, pp. 5817–5824.
- [17] Phani-Teja Singamaneni, Anthony Favier, and Rachid Alami. “Towards Benchmarking Human-Aware Social Robot Navigation: A New Perspective and Metrics”. In: *IEEE International Conference on Robot and Human Interactive Communication*. 2023.
- [18] Ada V. Taylor, Ellie Mamantov, and Henny Admoni. “Observer-aware legibility for social navigation”. In: *31st IEEE International Conference on Robot and Human Interactive Communication*. IEEE. 2022, pp. 1115–1122.
- [19] Gülhan Temel and Semra Erdogan. “Determining the sample size in agreement studies”. In: *Marmara Medical Journal* 30.2 (2017), pp. 101–112.
- [20] Qiping Zhang, Nathan Tsoi, Mofeed Nagib, Booyeon Choi, Jie Tan, Hao-Tien Lewis Chiang, and Marynel Vázquez. “Predicting Human Perceptions of Robot Performance during Navigation Tasks”. In: *ACM Transactions on Human-Robot Interaction* 14.3 (2025), pp. 1–27.